Dead-Zone-Free Atomic Magnetometry with Simultaneous Excitation of Orientation and Alignment Resonances

A. Ben-Kish and M. V. Romalis

Department of Physics, Princeton University, Princeton, New Jersey 08544, USA

(Received 2 January 2010; published 4 November 2010)

Atomic magnetometers have very high absolute precision and sensitivity to magnetic fields but suffer from a fundamental problem: the vectorial or tensorial interaction of light with atoms leads to ''dead zones,'' certain orientations of the magnetic field where the magnetometer loses its sensitivity. We demonstrate a simple polarization modulation scheme that simultaneously creates coherent population trapping (CPT) in orientation and alignment, thereby eliminating dead zones. Using ^{87}Rb in a 10 Torr buffer gas cell we measure narrow, high-contrast CPT transparency peaks for all orientations and also show the absence of systematic effects associated with nonlinear Zeeman splitting.

DOI: 10.1103/PhysRevLett.105.193601 PACS numbers: 42.50.Gy, 07.55.Ge, 32.30.Dx

Atomic magnetometers operate by measuring the Zeeman spin precession frequency and can achieve sensitivity surpassing even the best superconducting quantum interference devices (SQUID) [1]. They are particularly suitable for operation in Earth's magnetic field because measurements of the precession frequency can be performed with high fractional resolution, are related to the magnetic field only through fundamental constants, and are relatively insensitive to the orientation of the magnetometer. Atomic magnetometers are widely used for the most demanding applications, such as measurements of magnetic fields in space [2–4], mineral exploration [5], searches for archeological artifacts [6], and unexploded ordnance [7].

Since their inception 50 years ago, atomic magnetometers have suffered from a fundamental problem known as a ''dead zone'' [8]: for certain orientation of the magnetic field relative to the device the signal goes to zero. Dead zones are an inherent feature of the vector or tensor interactions used for optical pumping and detection of spin oscillations: for certain orientations the interaction term goes to zero. Previous solutions to this problem included using multiple magnetometer cells or beams [9,10], mechanical rotation of some components [11], and use of unpolarized light and spatially varying microwave fields [12]. Multiple interaction regions or slow mechanical rotation are used in all cases, presenting a problem for gradiometric measurements common to Earth-bound applications and requiring increased complexity for space-bound systems [3,4].

Here we demonstrate a dead-zone-free Rb magnetometer utilizing a *single* interaction region. The magnetometer uses a single laser beam with polarization modulation at the Zeeman frequency to simultaneously excite and detect the precession of the dipole and quadrupole (alignment and orientation) moments of the atomic density matrix. Because of the different vector nature of the two interactions, the transmission of the laser beam is sensitive to the magnetic field in any orientation.

Excitation of the magnetic resonance using light intensity modulation was first demonstrated by Bell and Bloom [13] and polarization modulation was explored in [14,15]. Magnetometry based on precession of alignment was extensively explored in nonlinear magneto-optical rotation magnetometers [16] while transmission monitoring has been used in CPT magnetometers [17–19]. However, in all of these cases the magnetometer signals go to zero for certain orientations of the magnetic field. Here we show that with a particular choice of light modulation parameters and detection method, one can realize a CPT magnetometer operating simultaneously on different coherences without any active adjustments, resulting in a large response for all orientations of the magnetic field.

In addition to avoiding dead zones our arrangement also largely eliminates ''heading errors,'' another long-standing problem, particularly for alkali-metal magnetometers. Heading errors are caused by nonlinear Zeeman splitting of the magnetic sublevels given by the Breit-Rabi formula. By using symmetric optical pumping with equal intensities of σ^+ and σ^- light we eliminate spin polarization along the magnetic field. The remaining third-order heading error [20] is suppressed by the square of the ratio of the Zeeman frequency to the hyperfine frequency. The error due to nuclear magnetic moment is also avoided by optical pumping on only one of the hyperfine ground states.

Consider light linearly polarized in the $\hat{x}$ direction with intensity I propagating parallel to the $\hat{z}$ axis, passing through a polarization modulator with an optic axis at 45° to $\hat{x}$ and a retardation angle $\phi = \phi_0 \cos\omega t$. The following Stokes parameters of the light will be modulated

$$S_1 = I\cos(\phi_0\cos\omega t), \tag{1}$$

$$S_3 = I\sin(\phi_0\cos\omega t). \tag{2}$$

The interaction of light with atoms can be written as an effective non-Hermitian ground-state Hamiltonian [21]

$$\langle n|H|m\rangle = \sum_{m'} \frac{\mathbf{E}^* \cdot \mathbf{d}_{nm'} \mathbf{d}_{m'm} \cdot \mathbf{E}}{\hbar(\omega_0 - \omega_{F,F'} + i\Gamma/2)}, \quad (3)$$

where $\mathbf{E}$ and $\mathbf{d}$ are the electric field and electric dipole operator, ω_0 is the laser frequency, $\omega_{F,F'}$ is the transition frequency from the ground state F to the excited state F', and Γ is the excited state decay rate. The Hamiltonian can be decomposed into a sum of scalar, vector and tensor components [21,22]. Retaining only terms proportional to the modulated Stokes parameters we obtain

$$H_{\mathrm{mod}} = \frac{2}{c\epsilon} \sum_{F,F'} \frac{\alpha^{(1)}_{F,F'} S_3 F_z + \alpha^{(2)}_{F,F'} S_1 (F_x^2 - F_y^2)}{\hbar(\omega_0 - \omega_{F,F'} + i\Gamma/2)}, \quad (4)$$

where $\alpha^{(1)}_{F,F'}$, $\alpha^{(2)}_{F,F'}$ are the vector and tensor atomic polarizability constants, respectively, defined in [22]. Light absorption in the vapor and the depopulation optical pumping rate are both proportional to the non-Hermition part of the Hamiltonian $H - H^\dagger$ [21,23,24]. In particular, for weak light intensity the atoms will develop orientation $\langle F_z \rangle \propto -S_3$ and alignment $\langle F_x^2 - F_y^2 \rangle \propto -S_1$ due to *depopulation* optical pumping. The effects of *repopulation* optical pumping are relatively small in the presence of buffer gas due to fast excited state spin relaxation.

The modulation of the Stokes parameters can be expanded in terms of Bessel functions:

$$S_1 = J_0(\phi_0) + 2\sum_{k=1}^{\infty} (-1)^k J_{2k}(\phi_0) \cos 2k\omega t, \quad (5)$$

$$S_3 = 2\sum_{k=0}^{\infty} (-1)^k J_{2k+1}(\phi_0) \cos(2k+1)\omega t. \quad (6)$$

One can see that for small ϕ_0 we get modulation of S_3 at ω and modulation of S_1 at 2ω. The Bell-Bloom (BB) magnetometer [13] [Fig. 1(a)] relies on the Larmor precession of the atomic orientation $\langle F_z \rangle$. If the frequency of the modulation ω matches the Larmor precession frequency ω_L, then $\langle F_z \rangle$ will be synchronously excited due to depopulation pumping by the modulation of S_3. The average transmission of the light through the cell will be increased due to the term $S_3 F_z \propto -\cos^2(\omega t)$. However, when the magnetic field is parallel to the $\hat{z}$ axis, $\langle F_z \rangle$ does not precess and the Bell-Bloom magnetometer has a dead zone for $\mathbf{B}$ parallel to the light direction. For this case, however, the alignment $\langle F_x^2 - F_y^2 \rangle$ will precess at $2\omega_L$ [Fig. 1(b)]. Hence, it can be synchronously excited by modulation in S_1 when $\omega = \omega_L$ and the transmission through the cell will increase due to the $S_1(F_x^2 - F_y^2) \propto -\cos^2(2\omega t)$ term. Thus, average transmission through the cell will exhibit a CPT transmission resonance at the same frequency $\omega = \omega_L$ for all orientations of the magnetic field.

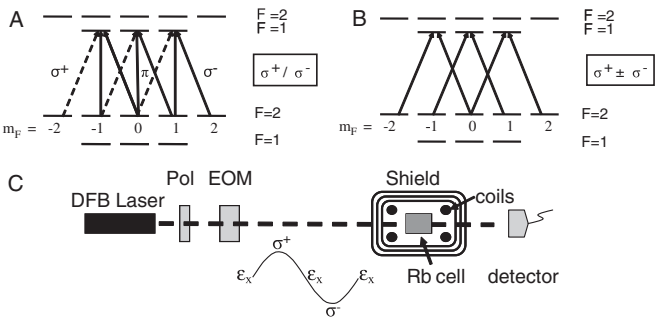

FIG. 1. Energy levels diagrams for Bell-Bloom magnetometer with σ^+ or σ^- polarized light (a), CPT magnetometer with linear $\sigma^+ \pm \sigma^-$ light (b), and the experimental apparatus (c).

The experimental apparatus and the atomic levels diagrams are presented in Fig. 1. A 795 nm DFB (distributed feedback) diode laser is used for excitation and detection of the $D1$ transition in ^{87}Rb. A linear polarizer and an electro-optic modulator (EOM) with its principle axes at 45° relative to the input polarization are used for generating the time dependent polarization modulation seen in Fig. 1. The modulated light is sent through a $2 \times 2 \times 5$ cm^3 glass cell with isotopically enriched ^{87}Rb metal and 10 Torr of N_2 buffer gas. The walls of the cell are coated with OTS coating and allow about 800 bounces before spin relaxation [25]. The cell is heated to 78 °C and is located inside a 3 layer μ-metal shield with a shielding factor of 10^4. A set of coils inside the shields is used for applying magnetic fields in any orientation. A set of gradient coils reduced magnetic field inhomogenuity. The transmitted light intensity through the cell is measured with a photodetector.

The wavelength dependence of the vector and tensor interactions for ^{87}Rb vapor in the presence of buffer gas and Doppler broadening has been considered in [24]. The imaginary part of H is maximized for both vector and tensor components close to the $F = 2 \rightarrow F' = 1$ $D1$ transition. The maximum of the scalar absorption also occurs near the same frequency; hence, the laser frequency can be locked to the transmission minimum.

The applied voltage on the EOM was set to oscillate sinusoidally with a retardation amplitude of approximately $\phi_0 \sim 2$ and the modulation frequency was scanned around the Larmor frequency ω_L. In order to check the response of the magnetometer to magnetic fields in any orientation, linear combinations of electric currents were sent to the three sets of coils inside the shields. An example of the measured transparency peak is shown in the inset of Fig. 2. The applied magnetic field was 28.6 mG, which corresponds to a Larmor frequency of 20 kHz. The contrast in this case is 50% and the FWHM of the CPT transmission resonance is 350 Hz. The measured contrast detected from each trace, for equally spread 58 orientations, was used for constructing the 3D plot in Fig. 2. Cubic spline interpolation was used for obtaining a clearer 3D view of the measured results. As shown in the 3D plot, there are no dead zones. One can also see that the measured contrast along the three major axes is different.

The natural axes of our scheme are set by the light propagation direction $\hat{k}_z$, the orientation of the linear polarization $\hat{\varepsilon}_x$, and the magnetic field. In the case of B_z field parallel to the propagation vector, the linear polarization

component of the light modulated at $2\omega_L$ generates CPT between appropriate Zeeman sublevels ($\Delta m = 2$) [Fig. 1(b)]. Destructive interference of the transition amplitudes in this Λ system will induce a transparency peak at resonance [17]. The BB signal is zero for this orientation. For a magnetic field oriented in a plane perpendicular to the propagation vector $\hat{k}_z$ (B_x, B_y), the circular polarization components (σ^+ or σ^-) modulated at the Larmor frequency (ω_L) will induce a BB transparency peak at the Zeeman resonance [$\Delta m = 1$, Fig. 1(a)]. With the quantization axis in the transverse plane the circularly polarized light can be thought of as "π" polarization and "$\sigma^+ \pm \sigma^-$" polarization generating a transparency peak resonance at ω_L. This orientation term will give a symmetric contribution to the transparency along B_x and B_y axes. In addition, the CPT resonance at $2\omega_L$ (alignment term) will also contribute to the signal in this plane. One can see from Eq. (4) that there are two dead zones in CPT resonance for magnetic field in $\pm\hat{x} \pm \hat{y}$ directions, as expected for a rank-2 tensor. For the B field at $\pm 45°$ to $\hat{x}$, the signal is entirely due to BB resonance. When both CPT and BB signals are present, their interaction is complicated by the fact that large spin orientation created by BB modulation also leads to a significant alignment. The sign of this contribution to the second term in Eq. (4) is opposite for magnetic field in $\hat{x}$ and $\hat{y}$ directions. As a result, CPT and BB resonances add constructively for B_y and destructively for B_x. By choosing an appropriate modulation depth and laser power one can adjust the relative strength of the two signals and make the ratio of maximum to minimum contrast to be approximately 3:1 while maximizing the overall contrast. Experimentally, we find the measured contrast ranges between 15%–60% while the FWHM is 350–700 Hz, without any dead zones, as seen in Fig. 2.

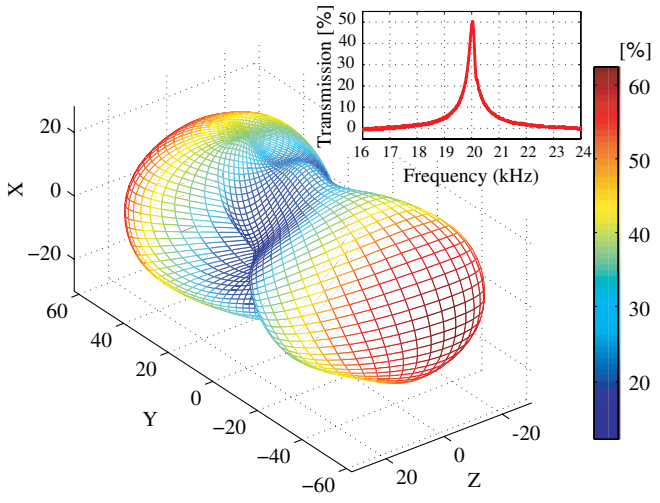

FIG. 2 (color). Contrast measurements as a function of magnetic field direction at 58 orientations, represented in percent of DC transmission. An example of the measured contrast in one orientation is shown in the inset.

In Fig. 3 detailed contrast measurements along the three major planes are shown. The upper set corresponds to the signal with both CPT and BB signals, with parameters similar to data in Fig. 2. The lower set is a reference measurement where the CPT contribution to the signal is eliminated by choosing a specific laser detuning to the midpoint between $F' = 1, 2$ upper levels. For this detuning the CPT signal is canceled due to different phase contribution of the two upper levels. It is evident that no signal is measured along the $\hat{z}$ axis in the BB scheme whereas this "dead zone" is totally avoided in the new scheme. Moreover, along one axis ($\hat{y}$), the signal's strength is larger and narrower than common BB magnetometers' signal, demonstrating a better signal to noise ratio.

The fast and balanced alternation between right and left circular polarization at the Larmor frequency also eliminates the heading error problem. The heading error, induced by an asymmetric illumination of the atoms, is manifested at magnetic fields on the order of Earth's magnetic field (~ 0.5 gauss) due to the nonlinear terms in the Breit-Rabi formula. In order to check this issue, we used the same experimental setup at higher magnetic fields. The EOM was driven at 1.9–2.2 MHz, corresponding to about 3 gauss for ^{87}Rb atoms. By working at a field which is $\sim$6 times Earth's magnetic field any distortion in the transparency due to the quadratic nature of the Breit-Rabi splitting should be observed.

The measured signal in Fig. 4 corresponds to a case where a 2.85 gauss magnetic field is tilted toward the Z axis by 26.5° from either the $\hat{x}$ or $\hat{y}$ axis. This compares signals with the largest possible contrast difference, corresponding to the sum and the difference of the BB and CPT

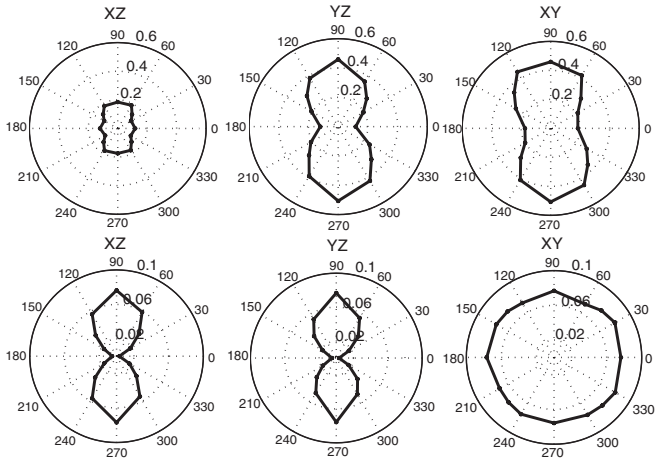

FIG. 3. Contrast measurements along the three major planes. Upper set corresponds to the new magnetometer. The lower set corresponds to a specific laser light detuning (see text) in which the CPT contribution to the signal is canceled and only "regular" Bell-Bloom contribution appears with a clear dead zone along the $\hat{z}$ axis. Note the factor of 6 difference in scales between the two sets and that the chosen laser detuning for canceling the CPT signal is not necessarily an optimized case for the BB contrast.

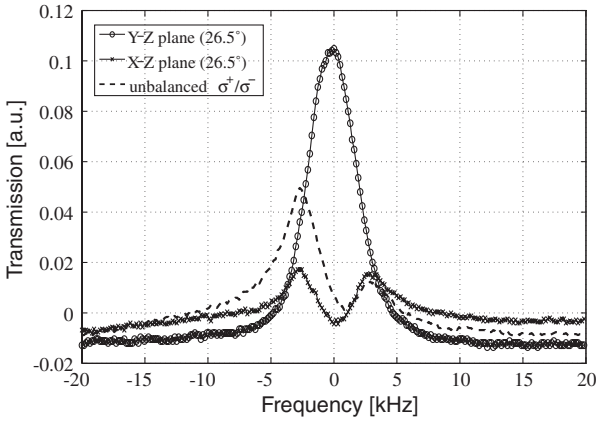

FIG. 4. The magnetometer's response at 2.85 gauss (2 MHz). The two symmetric traces correspond to a magnetic field tilted toward the $\hat{z}$ axis by 26.5° from the $\hat{x}$ or the $\hat{y}$ axis. The asymmetric signal (in the X-Z plane) corresponds to an unbalanced σ^+/σ^- contribution, obtained by inducing an additional bias to the EOM's driving voltage.

contributions. Whereas at low fields a single narrow peak is observed (e.g., Fig. 2), in this large field regime the Zeeman resonance is split into multiple peaks, particularly pronounced in the X-Z plane. The crucial observation here is that the signals are *centered* and *symmetric*. Therefore, changes between the strength of BB and CPT contributions associated with rotation of the magnetometer in an external field will not result in a shift of the central frequency.

In Fig. 4 we also present a case where unbalanced σ^+/σ^- contribution in the modulated light field is obtained by inducing an additional bias to the EOM's driving voltage. In this case the asymmetric signal will induce a heading error. This error is avoided in the current scheme due to the symmetric contribution of the various polarization components. In practice, one would also have to minimize residual polarization bias from stress-induced birefringence in various optical elements to obtain good suppression of heading errors.

In summary, a fundamental problem of ''dead zones'' in atomic magnetometers caused by the vectorial or tensorial interaction of the atomic polarizability with the light has been resolved by a simple polarization modulation scheme. Such a technique can be applied to both alkali-metal and metastable ^{4}He magnetometers [26]. We expect that the sensitivity of such magnetometer reaches picotesla level since measured CPT contrast ratio and linewidth are similar or better than in previous CPT magnetometers [18,19]. In the simplest implementation of the magnetometer, frequency modulation of the EOM excitation at a few hundred hertz can be used to lock to the maximum of the average transmission through the cell. It is also possible to improve the performance of the magnetometer by measuring the phase of the second and fourth harmonics of the Larmor frequency in the transmission signal, analyzing the polarization of the transmitted light, or using a separate probe laser. The amplitude of the EOM excitation can also be adjusted to maximize the signal for any given orientation of the magnetic field.

The heading errors specific to alkali-metal magnetometers in geomagnetic field are also largely eliminated due to symmetric optical pumping. Thus we expect that this technique will enable high precision isotropic magnetometry in many Earth-bound and space applications. Moreover, simultaneous controlled excitation of orientation and alignment by polarization modulation of a single light beam can be used to prepare specific atomic states for use in quantum information processing [27].

We thank Vishal Shah for assistance with the measurements and Tom Kornack and Scott Seltzer for fabricating the cell. This work was supported by ONR MURI.

[1] D. Budker and M. Romalis, Nature Phys. **3**, 227 (2007).
[2] M. Dougherty *et al.*, Space Sci. Rev. **114**, 331 (2004).
[3] S. Matousek, Acta Astronaut. **61**, 932 (2007).
[4] E. Friis-Christensen, H. Lühr, and G. Hulot, Earth Planets Space **58**, 351 (2006).
[5] M. Nabighian *et al.*, Geophysics **70**, 33ND (2005).
[6] A. David *et al.*, Antiquity **78**, 341 (2004).
[7] H. Nelson, J. McDonald, and D. Wright, Tech. Rep., NRL Report No. NRL/MR/6110–05-8874, 2005.
[8] A. L. Bloom, Appl. Opt. **1**, 61 (1962).
[9] B. Cheron *et al.*, J. Phys. III (France) **7**, 1735 (1997).
[10] B. Chéron, H. Gilles, and J. Hamel, Eur. Phys. J. Appl. Phys. **13**, 143 (2001).
[11] C. Guttin, J. Leger, and F. Stoeckel, J. Phys. IV (France) **4**, C4-655 (1994).
[12] E. B. Aleksandrov, A. K. Vershovskii, and A. S. Pazgalev, Tech. Phys. **51**, 919 (2006).
[13] W. E. Bell and A. L. Bloom, Phys. Rev. **107**, 1559 (1957).
[14] H. Gilles, J. Cheron, and J. Hamel, Opt. Commun. **81**, 369 (1991).
[15] H. Klepel and D. Suter, Opt. Commun. **90**, 46 (1992).
[16] D. Budker *et al.*, Rev. Mod. Phys. **74**, 1153 (2002).
[17] A. Nagel *et al.*, Europhys. Lett. **44**, 31 (1998).
[18] M. Stahler *et al.*, Europhys. Lett. **54**, 323 (2001).
[19] P. D. Schwindt *et al.*, Appl. Phys. Lett. **85**, 6409 (2004).
[20] S. J. Seltzer, P. J. Meares, and M. V. Romalis, Phys. Rev. A **75**, 051407(R) (2007).
[21] W. Happer, Rev. Mod. Phys. **44**, 169 (1972).
[22] J. M. Geremia, J. K. Stockton, and H. Mabuchi, Phys. Rev. A **73**, 042112 (2006).
[23] W. Happer and B. S. Mathur, Phys. Rev. **163**, 12 (1967).
[24] B. S. Mathur, H. Y. Tang, and W. Happer, Phys. Rev. A **2**, 648 (1970).
[25] S. J. Seltzer and M. V. Romalis, J. Appl. Phys. **106**, 114905 (2009).
[26] H. Gilles, J. Hamel, and B. Cheron, Rev. Sci. Instrum. **72**, 2253 (2001).
[27] B. Wang and *et al.*, Phys. Rev. A **75**, 051801(R) (2007).